Supplemental material

Buczacki et al., https://doi.org/10.1084/jem.20171385

Data S1 contains summary RNAseq DE tables, phenotype signatures, additional drug data, PDO sequencing data, and raw experimental data and is included as a separate Excel document.

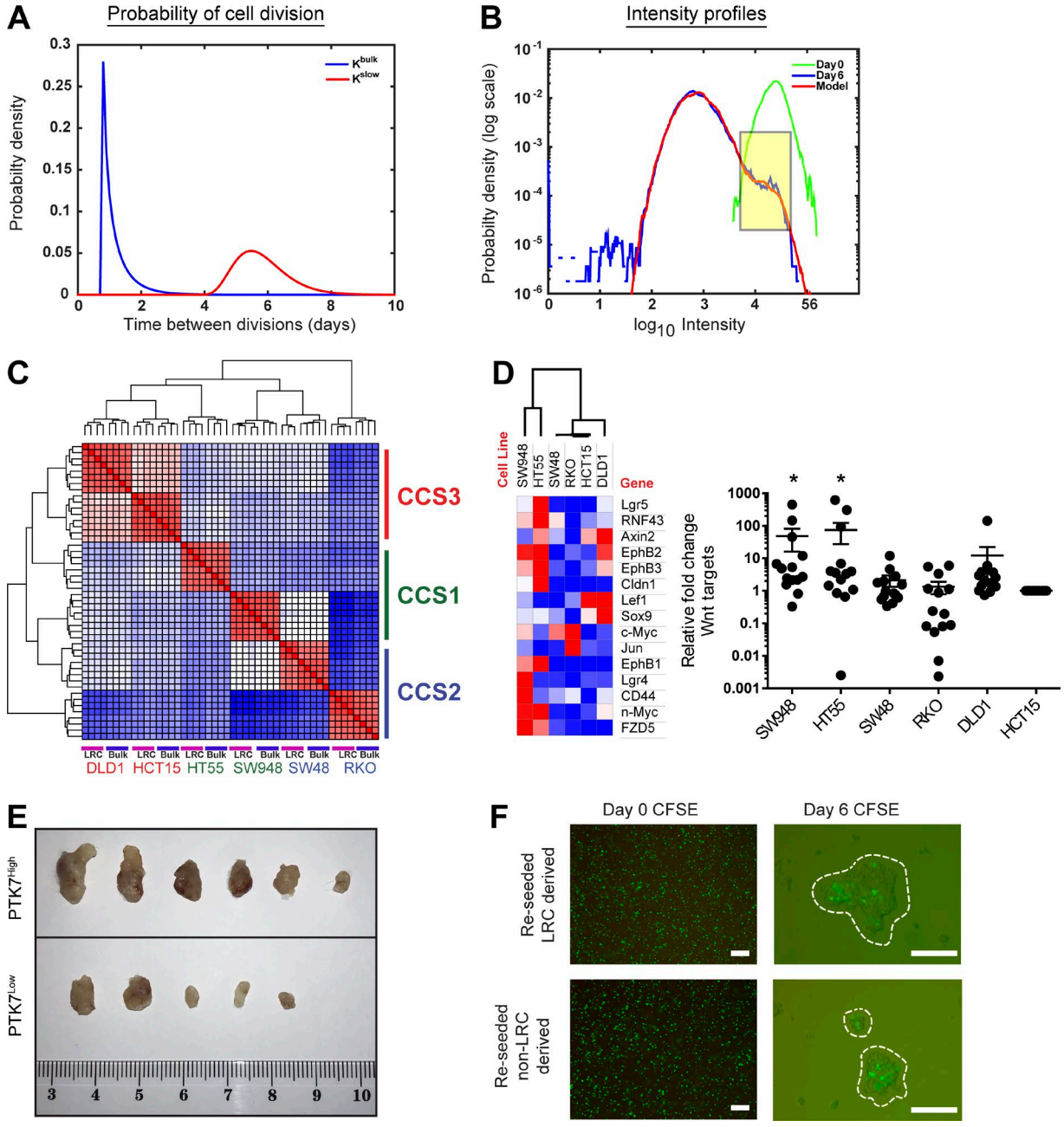

Figure S1. **Dormant CRC cells are contextually plastic. (A)** Optimum division time distributions for SW48 cells were calculated as described in Materials and methods, leading to a population making up the bulk of cells (blue) and a slowly cycling population (red). Distributions normalized to 1 for clarity. **(B)** Optimum CFSE model–generated intensity (red) was calculated as described in methods given an observed initial intensity at day 0 (green) and final intensity at day 6 (blue). A log scale is applied to each axis. Highlighted yellow box indicates the "kick," which identifies the slower cycling population in both simulated and real data. **(C)** Hierarchical clustering of RNAseq data from $CFSE^{High}$ (LRC) and $CFSE^{Bulk}$ (Bulk) from six CRC cell lines representing the three main subtypes. **(D)** Heat map with hierarchical clustering and accompanying dot plot of Wnt target gene expression levels in LRCs from the six CRC cell lines (red, up-regulated; blue, down-regulated). Expression levels in the dot plot are relative to HCT15-LRC levels. Mean ± SEM; *, $P < 0.05$ by one-way ANOVA. **(E)** Photograph of tumor xenograft sizes from SW948 FACS sorted $PTK7^{High}$ and $PTK7^{Low}$ spheroid cells. Ruler shows centimeter increments. **(F)** Fluorescent microscopy images of reseeded and CFSE-restained populations cultured as spheroids from LRCs and non-LRCs at initial seeding and 6 d later showing recapitulation of cell cycle hierarchies in derived spheroids. Bars, 100 µm.

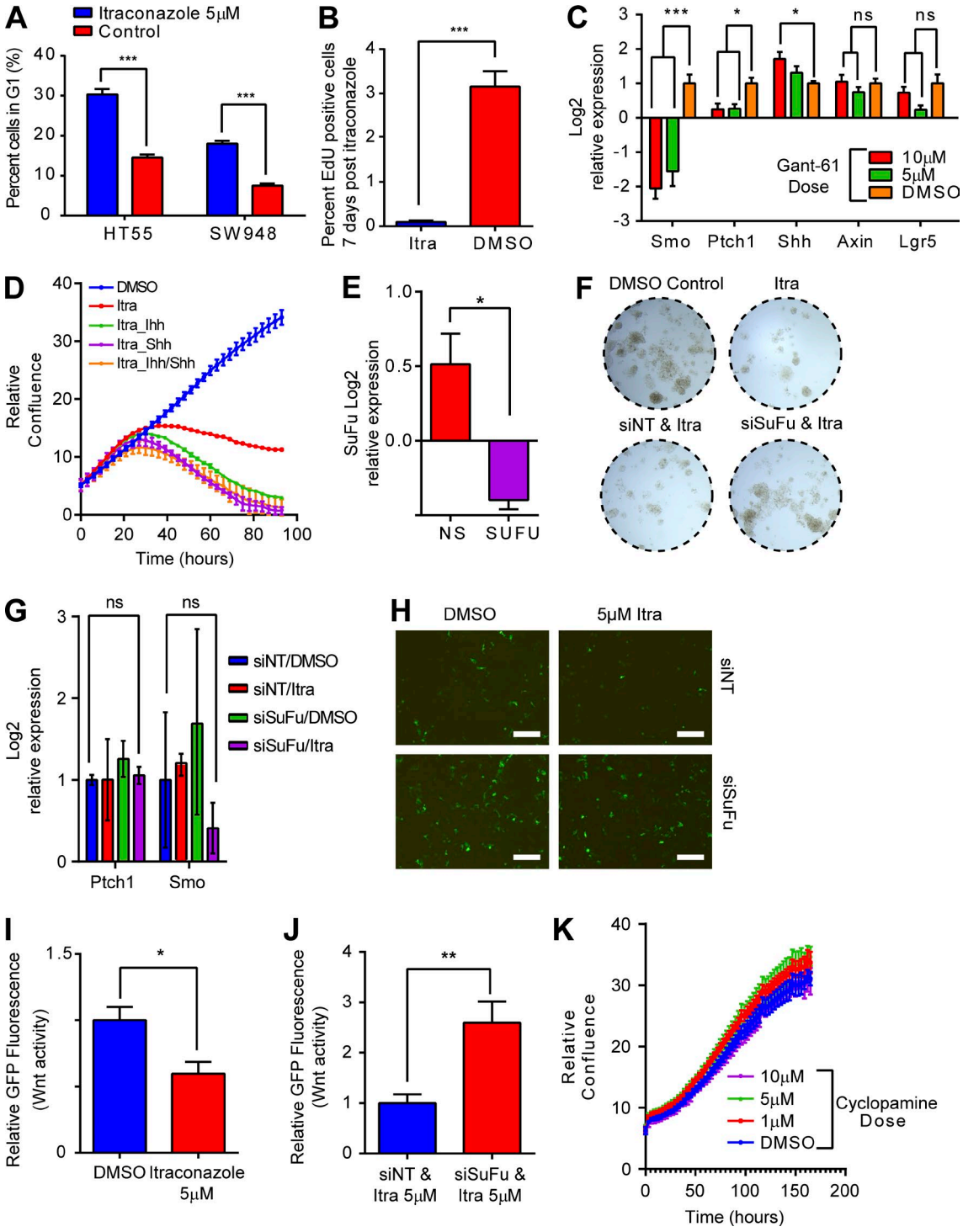

Figure S2. **Inhibition of SuFu-mediated Wnt activation drives the itraconazole phenotype. (A)** Histogram of the proportion of HT55 and SW948 cells arrested in G1, as determined by FACS analysis with PI staining, 48 h after itraconazole or DMSO control treatment and 24 h after labeling with EdU. ***, $P < 0.005$ by independent *t* tests on each cell line. **(B)** Histogram showing the proportion of EdU$^+$ SW948 cells 1 wk after treatment with itraconazole or DMSO control and 2 h after labeling with EdU. ***, $P < 0.005$ by unpaired *t* test. **(C)** RT-PCR data showing the response of SW948 cells to Gant-61 treatment. *, $P < 0.05$; ***, $P < 0.001$ by two-way ANOVA. **(D)** Live cell confluence graph showing recombinant Ihh (5 mg/ml) or Shh (7.5 mg/ml) fails to rescue the itraconazole phenotype in SW948 cells. **(E)** siRNA-mediated knockdown of SuFu reduces SuFu levels. *, $P < 0.05$ by unpaired *t* test. **(F)** Representative bright field images of SW948 cellular confluence after treatment with siSuFu, itraconazole, and controls. **(G)** Histogram of Hh target gene changes in response to itraconazole treatment. ns, not significant by two-way ANOVA. **(H)** Fluorescence microscopy images of GFP reporter activity in SW948 cells after transfection with TCF/LEF-GFP reporter construct, siNT, or siSuFu with and without itraconazole treatment. Bars, 100 μm. **(I)** FACS quantification of TCF/LEF-GFP fluorescence 48 h after itraconazole treatment and construct transfection. Data normalized to itraconazole-treated sample. *, $P < 0.05$ by unpaired *t* test. **(J)** FACS quantification of TCF/LEF-GFP fluorescence 48h after itraconazole treatment, siRNA, and construct transfection. **, $P < 0.05$ by unpaired *t* test. **(K)** Live cell confluence graph of the response of SW948 cells to cyclopamine. Itra, itraconazole. $n = 3$; mean ± SEM.

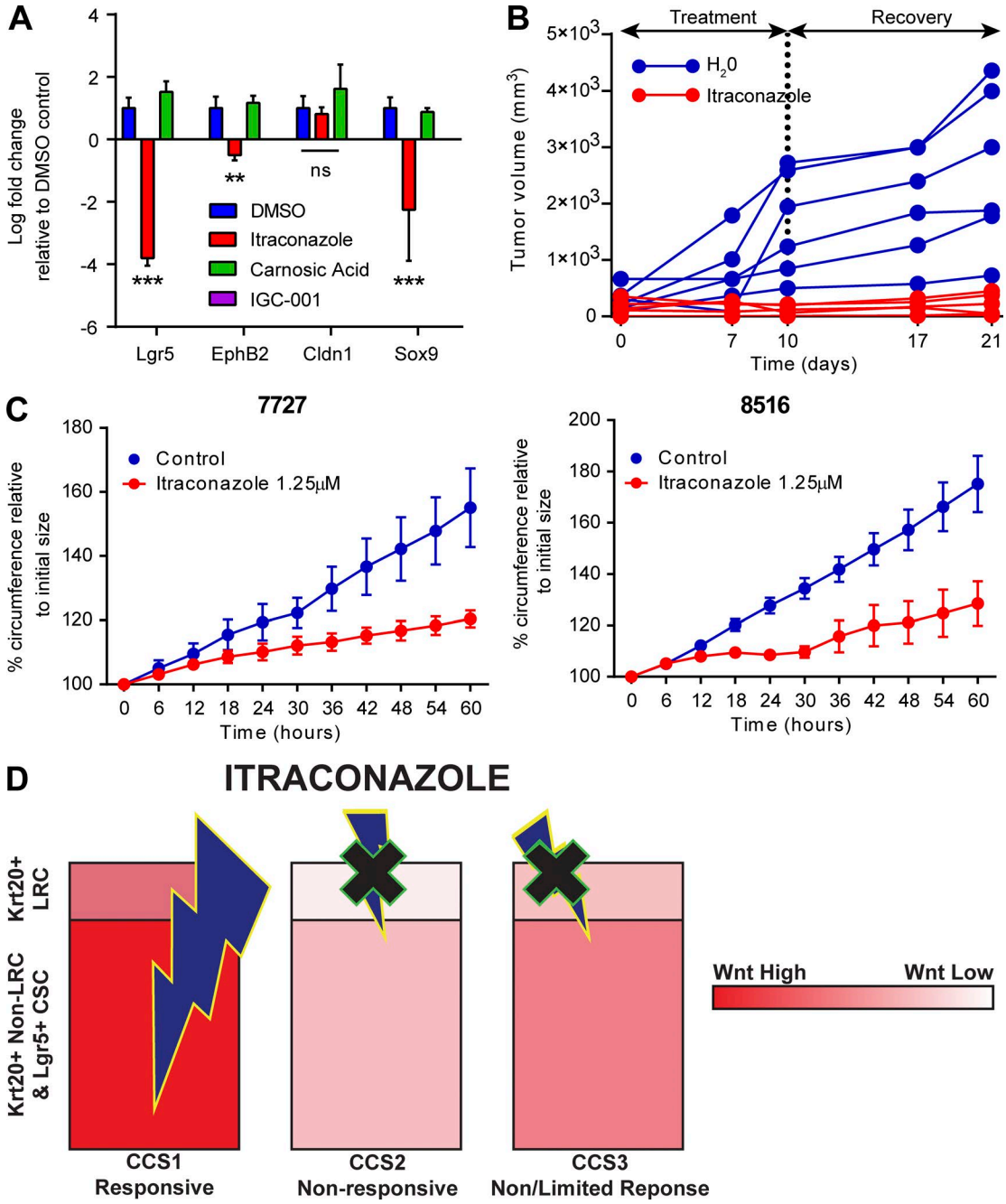

Figure S3. **The phenotype associated with itraconazole treatment is derived from Wnt inhibition. (A)** RT-PCR data showing changes in Wnt target gene expression in relation to treatment with DMSO control, itraconazole, and Wnt inhibtors carnosic acid and IGC-001. *n* = 4; mean ± SEM; ***, P < 0.001; **, P < 0.01 by two-way ANOVA. ns, not significant. **(B)** Graph showing the changes in tumor size of itraconazole-treated (red) or control-treated (H_20; blue) animals after establishment of SW948 xenografts and then after cessation of treatment. **(C)** Growth curves of the change in circumference of patient derived liver metastasis organoids with time after treatment with itraconazole for two further separate patient-derived lines. **(D)** Schematic representing the correlation in response to itraconazole with the molecular features of LRCs and non-LRCs across CRC subtypes.

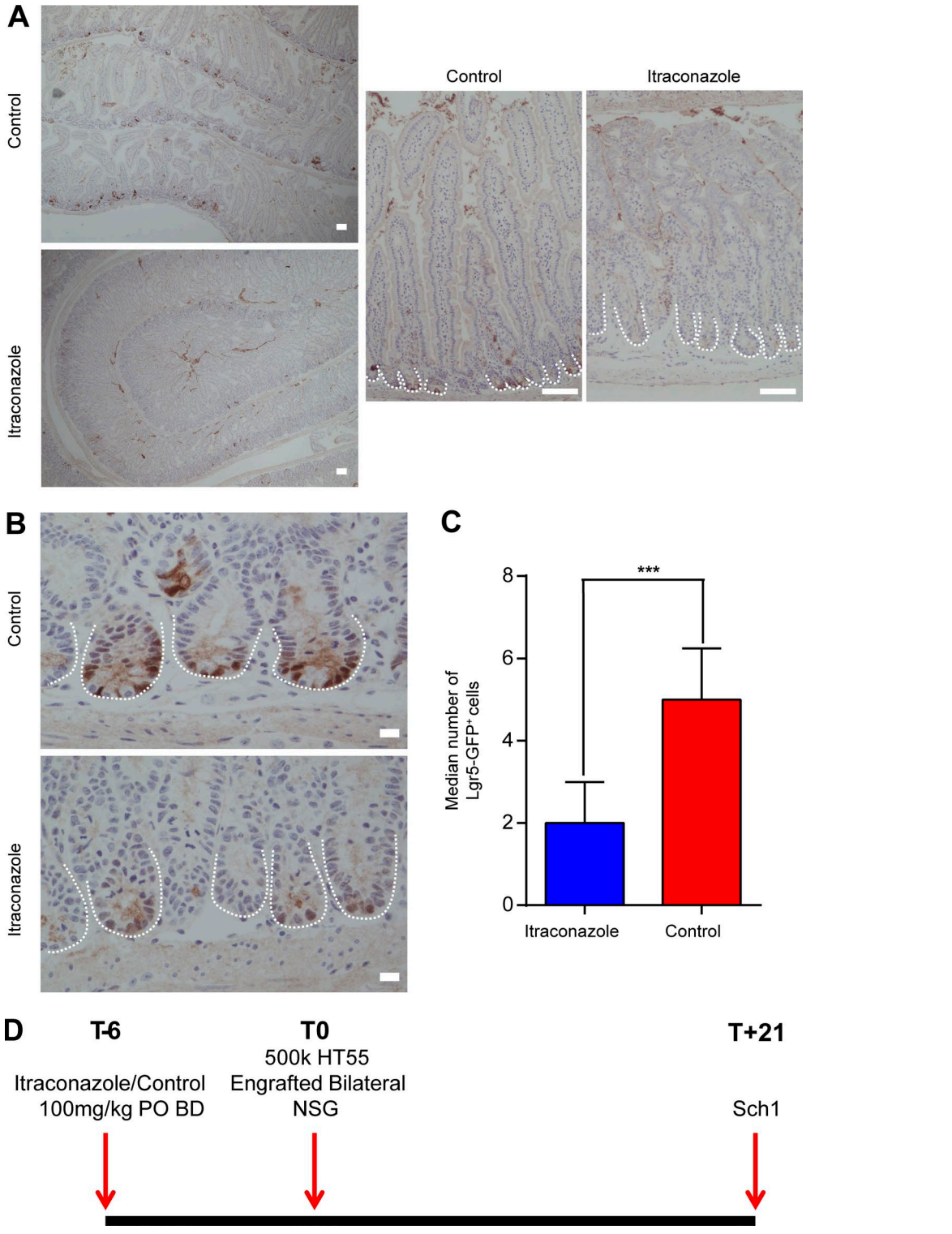

Figure S4. **In vivo, itraconazole diminishes the numbers of Lgr5-expressing intestinal stem cells. (A)** Bright field images of sections of small intestines from control and itraconazole-treated *Lgr5-Cre^{ER}_Apc$^{fl/fl}$* mice stained with anti-GFP antibody to identify Wnt-active Lgr5 stem cells. Bars, 100 µm. **(B)** Higher magnification images of A, demonstrating loss of expression of the Wnt target gene *Lgr5* in the base of small intestinal crypts. Bars, 10 µm. **(C)** Histogram showing the median number of GFP$^+$ cells per crypt in those with at least one identifiable GFP-expressing cell. $n = 50$; median ± interquartile range. ***, $P < 0.001$ by two-tailed Mann-Whitney test. **(D)** Schematic of the dosing and engraftment regimen of a 3 × 3 mouse comparison of the effects of itraconazole treatment on xenograft engraftment and growth. Mice were dosed with itraconazole (100 mg/kg) twice daily or water (10 ml/kg) for 6 d to reach steady-state serum levels. 500,000 HT55 cells were engrafted into the flanks bilaterally and mice monitored for tumor development. BD, bis in die (twice daily). PO, per os (by mouth).